LASER-ASSISTED CONTROL OF BISMUTH DOPING IN MAGNETIC NANOPARTICLES

[1,2]Ondrej HAVELKA, [1]Jan BRAUN, [1]Sabrin ABDALLAH, [1]Rafael TORRES-MENDIETA

[1]Institute for Nanomaterials, Advanced Technologies and Innovation, Technical University of Liberec, Liberec, Czech Republic, EU, ondrej.havelka@tul.cz, rafael.torres@tul.cz

[2] Faculty of Mechatronics, Informatics and Interdisciplinary Studies, Technical University of Liberec, Liberec, Czech Republic, EU

https://doi.org/10.37904/nanocon.2022.4578

Abstract

The fine control of mono- or bi-metallic nanoparticles' (NPs) chemical composition is one of the most critical concerns in nanomaterial manufacturing; however, when metals holding dissimilar characteristics form bi-metallic NPs, this becomes an unresolved matter. Herein we present the successful control of doping two different magnetic elements - nickel and iron- into bismuth to produce magnetic NPs with optical characteristics of semiconductors. For this, we have employed reactive laser ablation in liquids (RLAL) employing a magnetic foil (either nickel or iron) as the ablation target, which was immersed in an acetone solution with a hard-to-dissolve $Bi(NO_3)_3$ salt.

The employment of various $Bi(NO_3)_3$ concentrations showed that values between 0.01 and 1 mM are optimal for manipulating the doping degree on the NPs, which was verified by scanning electron microscopy. Moreover, their magnetic manipulation testing and inspection by ultraviolet-visible spectroscopy allowed assessing that the magnetic NPs formed by Bi doping of Fe display the most appropriate optical properties towards the material exploitation in photocatalysis. Furthermore, the minimal Bi salt employment resulted in chemical waste suppression verified by inductively coupled plasma spectroscopy. Since room conditions and no hazardous reducing agents were required for this synthetic procedure, the introduced alternative represents an up-and-coming practice for producing magnetic NPs doped by Bi.

Keywords: Nanoalloys, magnetic nanoparticles, bismuth compound, laser ablation in liquids, acetone

1. INTRODUCTION

By the end of the 20th century, nanotechnology had become a rapidly expanding field, continuing unabated over the years [1]. As a result, newly developed nanomaterials started to be employed in real applications outperforming the bulk materials from which they originated. This trend, moreover, did not end there; when nanomaterials formed by multiple elements started to be explored, it became evident that the arising new properties would be able to face the most demanding challenges our society faces. Therefore, a global effort began toward creating multi-element nanomaterials, which, by connecting multiple useful properties, gave rise to precious materials [2]. A clear example of this is NPs made up of two different metals, each providing a different type of particle behavior, like photonic and magnetic, which can be helpful in critical fields, such as photocatalysis. This widespread field has long been searching for recyclable materials that could be activated by the ubiquitous source of energy on our planet, sunlight radiation. In the past, magnetic Fe_3O_4/TiO_2 core-shell NPs were most often used for this purpose because they showed a suitable band gap and the possibility of being magnetophoretically recovered [3]. However, the main drawback of these magnetic NPs with a TiO_2 shell was, as in the case of pure TiO_2, the rapid recombination of photo-induced charge carriers and the promotion of catalytic reactions only by the ultraviolet (UV) part of the solar spectrum [4], representing only

4 % of the solar irradiance spectra. For this reason, the search for these recyclable materials with a bandgap capable of being activated by radiation falling in the solar irradiance visible (Vis) region, which is up to 10 times more abundant than the UV region, is crucial [5]. The state-of-the-art materials address such an issue by doping the TiO_2 side by plasmonic materials, which can transfer photo-induced charge carriers to TiO_2, expanding the material's ability to get activated by a broader part of the solar irradiance spectrum [6].

Although this is by itself an up-and-coming solution to overcome the TiO_2 optical limitations, TiO_2 is not the only photocatalyst under exploration. Other photocatalysts, like bismuth oxides also display wide band gaps, yet their slower charge recombination rate makes them even more interesting than TiO_2 [5]. Besides, unlike the TiO_2 case [3], doping bismuth-based photocatalysts' surfaces by transition metals as Ni or Fe can be of great benefit [7]. Specifically, by reducing the recombination rate of electron-hole pairs, thus, the photons used in photocatalysis remain available for the catalytic process longer.

Herein, we present a facile methodology to dope Ni or Fe by Bi oxide, which besides improving its electronic effects, expands its optical properties by narrowing its band gap, thus allowing it to utilize the sunlight irradiation spectrum more efficiently. Moreover, the ferromagnetic nature of the doped NPs provides it with magnetophoretic motility, which can serve for their reusability in photocatalytic reactions, preventing it from becoming waste after the first catalyst saturation, thus, making its use more sustainable [7]. Besides, to ensure complete materials sustainability, this work explores the synthesis of these doped NPs by RLAL, an eco-friendly laser-mediated route for multielement NPs preparation. In contrast to current multielement NPs synthesis techniques, RLAL enables their production without ligands and avoids hazardous chemicals usage, while ambient synthesis conditions are employed [8]. Thus, considering that this process enables the eco-friendly creation of NPs combining great optical and magnetic performance, we believe that the presented study will be of great importance in stimulating the generation of recyclable and sustainable photocatalysts with tailored optical properties.

2. EXPERIMENTAL

The NPs production consisted of irradiating a magnetic foil (nickel with > 99.98 % Ni, iron with > 99.99 % Fe, both from Sigma-Aldrich) immersed in a 40 mL acetone solution by pulsed laser radiation (Onefive Origami XP-S; output power 5.1 W, pulse duration < 400 fs, central wavelength 1030 nm). To get different elements' stoichiometries between Bi and the different magnetic elements within NPs, the $Bi(NO_3)_3 \cdot 5H_2O$ salt (> 99.999 %, Sigma-Aldrich) was dissolved in acetone at various concentrations (0, 0.01, 0.1, 1 mM), which range was based on a previous study conducted in aqueous media [9]. Note that larger concentration values were disregarded due to a massive laser beam scattering, which disabled production of magnetic NPs. The irradiation process followed the scheme displayed in **Figure 1**. In brief, a galvanometric mirror system (intelliscan 14; moving at a 2 m/s speed) was employed to move the focused laser beam by an F-Theta Lens (160 mm focal length) over the entire surface of the metallic foil while the Bi solution was magnetically stirred at 100 rpm. The employed laser and irradiation parameters were selected to maximize the NPs production rate (maximal average power: 5.1 W, optimized repetition rate: 0.7 MHz, optimized irradiation time: 20 min, scanning pattern: spiral). Note that the acetone volume was decreased on average by about 10 % to 36.1 mL due to the solvent heating-evaporation process caused by 20 min irradiation, which slightly influenced Bi salt concentration in the acetone during the NPs synthesis.

After the NPs preparation, the samples were cleaned of residual salt using a centrifuge (Centrifuge MiniSpin plus) for 15 minutes at 14500 rpm. The sediments obtained from the process were re-dispersed in Eppendorfs with fresh acetone by an ultrasonic cleaner (SONOREX DIGITEC DT 510 H, 35 kHz, 9.7 L). After the homogenization of samples, the magnetic NPs were collected on one side of Eppendorf using a neodymium magnet. The remaining non-magnetic material was removed. Then, the centrifugation followed by magnetic separation processes were done twice to ensure proper NPs cleaning.

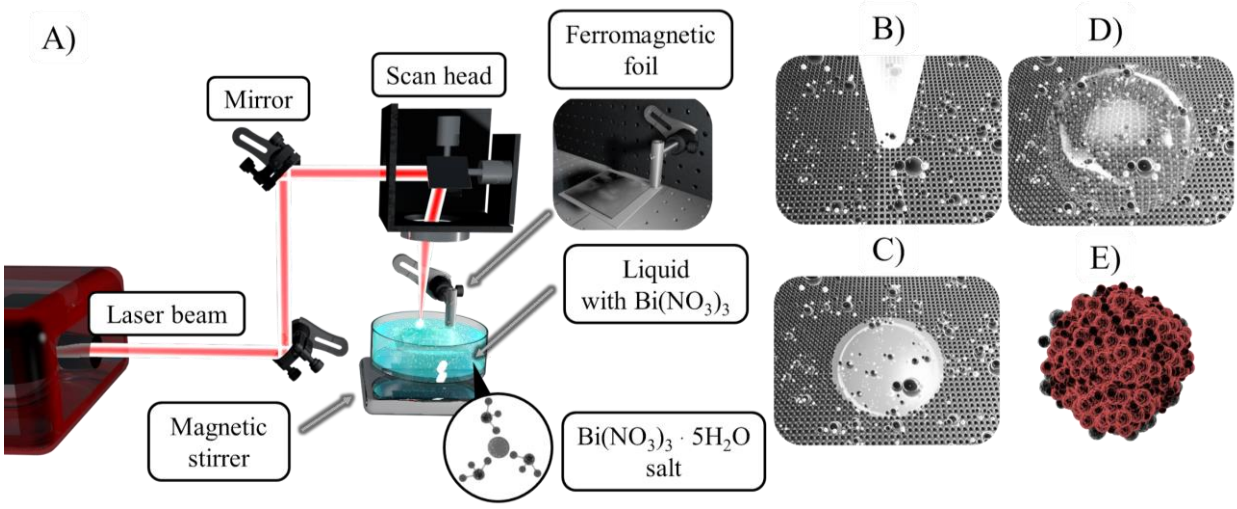

Figure 1 A) RLAL of an acetone-based solution of $Bi(NO_3)_3 \cdot 5H_2O$ and magnetic foil consisting of B) laser irradiation of a foil immersed in a solution, C) creation of the plasma from metal species and dissociated liquid molecules, D) cavitation bubble evolution, from which are E) formed bimetallic NPs released after bubble‘s collapse.

After the cleaning process, the samples‘ element composition was analyzed by an inductive-coupled plasma mass spectroscope (ICP-MS; NexION 3000D, Perkin Elmer) and optical emission spectroscope (ICP-OES; Optima 2100Dv, Perkin Elmer). Besides, the samples' morphology, size distribution, and chemical composition were then determined using a scanning electron microscope (FE-SEM; UHR Carl Zeiss Ultra Plus, Jena) equipped with an energy dispersive X-ray detector (EDX; Oxford X-Max 20). Finally, the optical features of samples were assessed by a UV-Vis spectroscope (PerkinElmer Lambda 35, Perkin Elmer) in a wavelength range from 230 to 800 nm and at a wavelength resolution of 1 nm.

3. RESULTS AND DISCUSSION

3.1. ICP-MS and ICP-OES

The NPs element compositions obtained after simple purification by centrifugation and after the entire cleaning process, including the magnet, can be found in **Table 1**. For simplicity, the samples are marked as S1-S8 according to the table. The results showed that, in general, the mass fraction of each element in the synthesized particles is proportional to the concentration of the Bi salt solution, while all or most of the salt is consumed in the synthesis. At the same time, the magnetically cleaned samples displayed a slightly higher Bi content. It is, at first sight, non-intuitive due to the possible formation of NPs with no or low magnetic element content or to the incomplete separation of redundant Bi salt during the centrifugation process. Since the location (not just the amount) of bismuth in the structure of NPs can play a crucial role in their magnetic response, further analysis of the NPs' internal structure is needed. Moreover, although there is a material loss, after magnet-assisted purification, minimally 93 % of NPs were recovered, indicating most of the material holds the desired magnetic properties. This result is especially significant in the case of Fe-based samples, in which >99 % NPs recovery rate indicates a better Fe doping by Bi. Although, according to the Hume-Rothery rules [10], neither Bi-Fe nor Bi-Ni are element combinations able to produce substitutional alloys, Bi and Fe share a property that may help them form a more stable system; both elements can be arranged in a cubic crystal centered in the body. This can enable a more efficient Bi allocation in the crystal formed by Fe, thus, leading to better element doping without compromising the inherent Fe magnetophoretic motility properties, which can be beneficial, for instance, for the magnetic recovery of NPs after their use in catalysis.

Table 1 Chemical composition of laser-prepared colloids. Average weight percentage of Bi, Ni, Fe in the no-magnetically purified and magnetically purified samples determined by ICP-MS, ICP-OES.

Sample No	Foil	No-magnetically purified			Magnetically purified			Magnetically recovered NPs (%)
		Salt (mM)	Bi (wt%)	Ni/Fe (wt%)	Salt (mM)	Bi (wt%)	Ni/Fe (wt%)	
S1	Ni	0	0	100	0	0	100	-
S2		0.01	2.7	97.3	0.01	3.3	96.7	97.5
S3		0.1	13.8	86.2	0.1	19.4	80.6	98.0
S4		1	88.6	11.4	1	94.2	5.8	92.9
S5	Fe	0	0	100	0	0	100	-
S6		0.01	2.8	97.2	0.01	4.2	95.8	99.0
S7		0.1	18.6	81.4	0.1	19.8	80.2	99.3
S8		1	66.5	33.5	1	72.2	27.8	99.1

3.2. SEM

The SEM micrographs displayed in **Figure 2** show a significant morphological difference in the Fe- and Ni-based NPs (samples S4 and S8 were selected as their difference is most evident). As anticipated by ICP data, there is a lower mixing of Ni and Bi, where, as indicated by EDS mapping, Bi is in fact found in the form of separated NPs clusters accompanied by residues of the Bi salt. In contrast, the element mapping of the Fe-based sample exhibited a homogeneous distribution of both elements, indicating an excellent mixture. Although its micrograph reveals an agglomeration of NPs with similar average size, there are large-looking NPs decorated by smaller ones as well. This is a result that, even when it can be further corroborated by TEM analysis, largely agrees with the previous observation that in nanoalloys with segregated phases, the element more affine to the solvent used in the synthesis tends to migrate to the outermost part of the NPs [11,12]. In our case, the acetone represents a solvent, which can enable the separation of Bi to the desired outermost part due to the $Bi(NO_3)_3$ affinity to acetone [13].

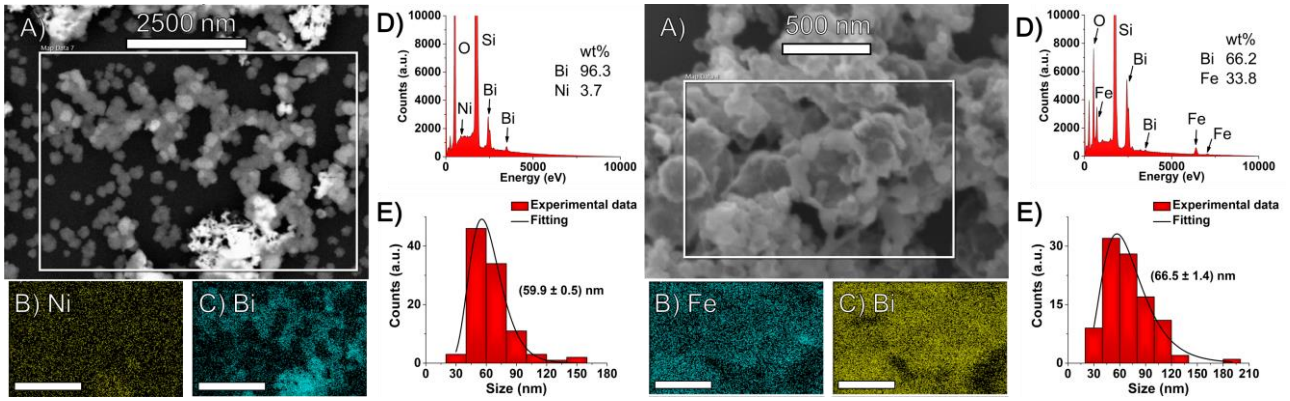

Figure 2 Representative SEM (left side - S4, right side - S8), A) micrograph, B) magnetic element and C) Bi EDX mapping with D) corresponding spectrum, and E) NPs size histogram fitted with the log-normal distribution.

3.3. Optical properties

Based on the solar irradiance spectra comparison with the samples' band gap, which was calculated according to the Tauc plot [14,15], the most promising sample was S8. This sample exhibited a unique band gap position

at 2.6 eV (**Figure 3**), approaching the blue (Vis) part of the solar irradiance, which is the most intensive part of spectra during sunny days and the noon daylight illumination [16].

Moreover, the sample displays a secondary band gap at 3.7 eV, which is typical for Bi oxide forms used in photocatalysis [17]. According to the NPs morphology revealed by SEM analysis, this double band gap behavior can be a consequence of the NPs surface alternating between Fe and Bi elements. Thus, providing the NPs with the possibility to be activated by either visible or UV light, expanding the capabilities of Bi-based photocatalysts for using the sunlight radiation more efficiently.

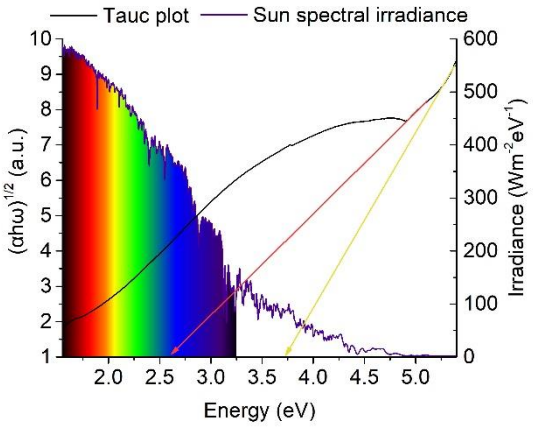

Figure 3 Comparison of Sun spectral irradiance during periods of moderate solar activity [18] with Tauc plot of S8 sample showing the proximity of Sun irradiance maximum and band gap position of synthesized NPs (red line), while the remaining Bi-related band gap (orange line) present in S8 meets the UV part of the solar spectra.

4. CONCLUSION

The current study reveals that RLAL methodology enables the production of Fe- and Ni-based magnetic NPs doped by Bi. Moreover, the control of Bi precursor concentration directly affects the doping degree found in the NPs, where Fe shows the best affinity for the allocation of Bi. Since these two elements forming a phase segregated nanoalloy are also found as alternating in the NP's surface, the produced NPs are capable of displaying two band gaps, one at the Vis region and one at the UV region of the sunlight radiation spectrum. This implies that the doping of Fe by Bi not only leads to the production of a semiconductor with the ability to be activated by visible and UV radiation, but its magnetophoretic motility inherited from Fe turns it into a recyclable, and because of this, a very valuable alternative towards photocatalysis. Finally, since the current synthesis approach largely minimizes chemical waste production, it is considered that the current results will be of fundamental importance for the future development of potent and magnetically recyclable photocatalysts.

ACKNOWLEDGEMENTS

The research presented in this article was supported by the Internal Grant of the Technical University of Liberec (SGS-2022-3008) and the Ministry of Education, Youth and Sports in the Czech Republic under the Research Infrastructures NanoEnviCz (Project No. LM2018124).

REFERENCES

[1] ROCO, Mihail C. The long view of nanotechnology development: the National Nanotechnology Initiative at 10 years. In: *Nanotechnology research directions for societal needs in 2020*. Springer, Dordrecht, 2011, pp. 1-28.

[2] FERRANDO, Riccardo; JELLINEK, Julius; JOHNSTON, Roy L. Nanoalloys: from theory to applications of alloy clusters and nanoparticles. *Chemical reviews*, 2008, vol. 108, no. 3, pp. 845-910.

[3] ÁLVAREZ, Pedro M., et al. Preparation and characterization of magnetic TiO2 nanoparticles and their utilization for the degradation of emerging pollutants in water. *Applied Catalysis B: Environmental*. 2010, vol. 100, no.1-2, pp. 338-345.

[4] WEI, Zhidong; LIU, Junying; SHANGGUAN, Wenfeng. A review on photocatalysis in antibiotic wastewater: Pollutant degradation and hydrogen production. *Chinese Journal of Catalysis*. 2020, vol. 41, no. 10, pp. 1440-1450.

[5] PELAEZ, Miguel, et al. A review on the visible light active titanium dioxide photocatalysts for environmental applications. *Applied Catalysis B: Environmental*. 2012, vol. 125, pp. 331-349.

[6] BIELAN, Zuzanna, et al. Defective TiO2 core-shell magnetic photocatalyst modified with plasmonic nanoparticles for visible light-induced photocatalytic activity. *Catalysts*. 2020, vol. 10, no. 6, pp. 672.

[7] REN, Ao, et al. Enhanced visible-light-driven photocatalytic activity for antibiotic degradation using magnetic NiFe2O4/Bi2O3 heterostructures. *Chemical engineering journal*. 2014, vol. 258, pp. 301-308.

[8] FRIAS BATISTA, Laysa M., et al. Generation of nanomaterials by reactive laser-synthesis in liquid. *Science China Physics, Mechanics & Astronomy*, 2022, vol. 65, no. 7, pp. 1-45.

[9] ETTEL, David, et al. Laser-synthesized Ag/TiO nanoparticles to integrate catalytic pollutant degradation and antifouling enhancement in nanofibrous membranes for oil-water separation. *Applied Surface Science*. 2021, vol. 564, pp. 150471.

[10] MIZUTANI, Uichiro. Hume-Rothery rules for structurally complex alloy phases. *MRS Bulletin*. 2012, vol. 37, no. 2, pp. 169-169.

[11] ETTEL, David, et al. Expansion of Optical Properties in Tiox Nanoparticles by their Laser-Mediated Alloying with Ag. *Education*. 2020, pp. 109-115.

[12] JOHNY, Jacob, et al. Multidimensional thermally-induced transformation of nest-structured complex Au-Fe nanoalloys towards equilibrium. *Nano Research*. 2022, vol. 15, no.1, pp. 581-592.

[13] OLLEVIER, Thierry, JALBA, Angela and KEIPOUR, Hoda. Bismuth(III) Nitrate Pentahydrate. *In Encyclopedia of Reagents for Organic Synthesis*, 2016.

[14] TAUC, Jan. Optical properties and electronic structure of amorphous Ge and Si. *Materials research bulletin*. 1968, vol. 3, no. 1, pp. 37-46.

[15] MAKUŁA, Patrycja; PACIA, Michał; MACYK, Wojciech. How to correctly determine the band gap energy of modified semiconductor photocatalysts based on UV-Vis spectra. *The Journal of Physical Chemistry Letters*. 2018, vol. 9, no. 23, pp. 6814-6817.

[16] TAYLOR, A. H.; KERR, G. P. The distribution of energy in the visible spectrum of daylight. *JOSA*. 1941, vol. 31, no.1, pp. 3-8.

[17] GBASHI, Kadhim R., et al. Structural, morphological, and optical properties of nanocrystalline (Bi2O3) 1− x:(TiO2) x thin films for transparent electronics. *Plasmonics*. 2019, vol. 14, no. 3, pp. 623-630.

[18] GUEYMARD, Christian A. The sun's total and spectral irradiance for solar energy applications and solar radiation models. *Solar energy*. 2004, vol. 76, no. 4, pp. 423-453.